Elastic properties and spectroscopic studies of fast ion conducting Li$_2$O–ZnO–B$_2$O$_3$ glass system

C. Narayana Reddy [a], R.P. Sreekanth Chakradhar [b,*]

[a] *Department of Physics, P.E.S. College, Bangalore University, Bangalore 560050, Karnataka, India*
[b] *Glass Technology Laboratory, Central Glass & Ceramic Research Institute, Kolkata 700032, West Bengal, India*

Abstract

Glass systems of the composition xLi$_2$O–20ZnO–(80 − x)B$_2$O$_3$ where (x = 5, 10, 15, 20, 25 and 30 mol%) have been prepared by melt quenching technique. Elastic properties, ^{11}B MAS-NMR and IR spectroscopic studies have been employed to study the structure of Li$_2$O–ZnO–B$_2$O$_3$ glasses. Elastic properties have been investigated using sound velocity measurements at 10 MHz. Elastic moduli reveal trends in their compositional dependence. The bulk modulus and shear modulus increases monotonically with increase of BO$_4$ units, which increase the dimensionality of the network. ^{11}B MAS-NMR and IR spectra show characteristic features of borate network and compositional dependent trends as a function of Li$_2$O/ZnO concentration. The results are discussed in view of borate network and the dual structural role of Zn^{2+} ions. The results indicate that the Zn^{2+} are likely to occupy network-forming positions in this glass system.
© 2006 Elsevier Ltd. All rights reserved.

Keywords: A. Amorphous materials; C. Nuclear magnetic resonance; C. Ultrasonic measurements; C. Differential scanning calorimetry; C. Infrared spectroscopy; D. Elastic properties

1. Introduction

Borate glasses containing Li$^+$ have been extensively studied due to their technological applications in solid-state batteries [1]. Small size, light weight and highly electro-positive character of lithium ions are considered as factors which give raise to high energy densities [2]. Dependence of conductivities of these glasses has been examined to understand the influence of structure, stability and compositions on their ion conduction [3]. Alkali borate glasses have been extensively studied over the years to elucidate the nature and relative concentration of various borate units constituting the glass network. Boron atoms in these glasses are both three and four coordinated to oxygens and are generally designated as B$_3$ and B$_4$ units. B$_3$ units may be represented as [BO$_{3/2}$]^0 = B$_3$ or charged [BO$_{2/2}$O]$^-$ = B$_2$ while B$_4$ may be represented as [BO$_{4/2}$]$^-$. The various borate units can often give rise to tightly organized structures resulting in intermediate order. The concentration of the various borate species in the glass structure is however determined by the nature and concentration of the modifier oxides. The ^{11}B NMR [4–6] and the IR [7–10] investigations play important role in identifying several borate groups consisting of boron–oxygen triangles and tetrahedra, which forms the glass network at various modification levels.

* Corresponding author.
   E-mail addresses: chakra@cgcri.res.in, sreechakra72@yahoo.com (R.P.S. Chakradhar).

Higher valent oxides, such as MO (where M = Zn, Mg, Pb, etc.) when used as modifiers, the cations also produce important structural effects due to the higher valent cations. There are important reports in literature [3,5], which suggests that, Zn^{2+}, Mg^{2+}, Pb^{2+}, etc., occupy both network-forming and network modifying positions. The pressure dependence studies of Na^+ ion conductivity on Na_2O–ZnO–B_2O_3 glass have also indicated that the Zn^{2+} ions prefer network-forming positions [11]. The dual role of divalent ions is not only seen in borate glasses but also in silicate and phospho-molybdate glasses and these aspects have been thoroughly investigated by using various techniques [12].

Among the various experimental methods available for studying structure–property relations, elastic properties of solid materials are of considerable significance. Because, their measurement yields information concerning the forces that are operative between the atoms or ions comprising solid. This is fundamentally important in interpreting and understanding the nature of bonding in the solid-state. Therefore, the choice of the most appropriate material for particular application requires knowledge of its mechanical properties. Hence, elastic properties are suitable for describing the glass structure as a function of composition [13]. There have been studies and reports [14–16] on several binary alkali borate glasses, which show that there is a correlation between elastic properties and borate glass structure. In Na_2O–B_2O_3 glass system [17], the elastic properties have been discussed in terms of boron coordination. The elastic properties of various borate glasses have also been reported [18–21]. In this paper, we present elastic property measurements of the ternary system, viz., lithium–zinc–borate glasses and their dependence on Li_2O and ZnO concentrations. The present studies attempt to correlate the changes in elastic moduli to the anticipated structural changes in the borate network.

2. Experimental

The glass samples of the general formula xLi_2O–$20ZnO$–$(80 - x)B_2O_3$ where (x = 5, 10, 15, 20, 25 and 30 mol%) have been prepared by the melt quenching technique. Required quantities of Analar grade lithium carbonate (Li_2CO_3), zinc oxide (ZnO) and orthoboric acid (H_3BO_3) were mixed together by grinding the mixture repeatedly to obtain a fine powder. The mixture is melted in porcelain crucible at about 1473 K for about 30 min to homogenize the melt. Glasses were obtained by quenching the melt between two brass plates. For ultrasonic measurements a special sample mould was fabricated of dimension 10 mm in diameter and 12 mm in length. The cylindrical shaped samples were obtained for ultrasonic measurements by quenching the melt in a brass mould, which was preheated (about 423 K) to avoid breaking of the samples due to thermal strains. To characterize the samples X-ray diffractogram studies have been carried out, the spectra did not show any sharp peaks, indicating that the samples were amorphous in nature. The glass transition temperature (T_g) was measured using a Perkin-Elmer DSC-2 Differential Scanning Calorimeter. The measurements were carried out at a heating rate of 10 K/min. All the samples were annealed below their glass transition temperature and preserved under anhydrous atmosphere. The densities of glasses were measured using toluene as an immersion liquid (density = 0.86 g/cm^3 at 27 °C). Molar volume (MV) has been calculated from the molecular weight (M) and density (ρ) using the relation, MV = M/ρ. The samples were polished to get uniform thickness and flat parallel surfaces of optical finish.

The samples were crushed to fine powder and ^{11}B MAS-NMR spectra were recorded with a Bruker MSL-300 solid-state high-resolution spectrometer operating at 96.28 MHz. The chemical shift values were recorded with respect to the resonance signal of BF_3 Et_2O. The IR spectra of freshly prepared glass samples were recorded on a Perkin-Elmer 580 Double Beam IR Spectrometer (300–2000 cm^{-1}) using KBr pellet at room temperature.

2.1. Sound velocity measurements

Ultrasonic velocity measurements were carried out at room temperature with a frequency of 10 MHz using x-cut and y-cut quartz transducers. A pulse superposition technique was employed using ultrasonic interferometer. Salol (phenyl salicilate) was used as a bonding material between the glass samples and transducers. Using Mcskimin's δt criteria the round trip delay time 't' has been calculated [22,23]. By measuring the thickness of the sample (d), longitudinal (V_l) and transverse (V_t) wave velocities were calculated using the relation,

$$V = \frac{2d}{t}.$$

The various elastic properties of the glasses investigated were calculated using the following relations:

$$\text{Longitudinal modulus}, L = \rho V_l^2 \tag{1}$$

$$\text{Shear modulus}, G = \rho V_t^2 \tag{2}$$

$$\text{Bulk modulus}, K = L - \tfrac{4}{3}G \tag{3}$$

$$\text{Young's modulus}, E = (1 + \sigma)2G \tag{4}$$

$$\text{Poisson's ratio}, \sigma = \frac{L - 2G}{2(L - G)} \text{ and} \tag{5}$$

$$\text{Debye temperature}, \theta_D = \frac{h}{k}\left[\frac{3\rho q N_A}{4\pi M}\right]^{1/3} V_m, \tag{6}$$

$$\frac{3}{V_m^2} = \frac{1}{V_l^3} + \frac{1}{V_t^3}. \tag{7}$$

where L, G, K and E are longitudinal, shear, bulk and Young's modulus, respectively, ρ the density, σ the Poisson's ratio, θ_D the Debye temperature, h the Plank's constant, k the Boltzman's constant, q the charge per unit formula, N_A the Avogadro number, M the molecular weight and V_m is the mean sound velocity.

3. Results and discussions

Table 1 lists the glass code, composition, density, molar volume and glass transition temperature of the investigated glasses. The sound velocity, elastic moduli, Poisson's ratio and Debye temperature are listed in Table 2.

3.1. Density, molar volume and glass transition temperature

The variation of density and molar volume is shown in Fig. 1. As can be seen from figure the density increases monotonically while the molar volume decreases with the increase of Li_2O concentration. The variation of density with Li_2O concentration can be explained by considering the structural changes occurring in the coordination of boron glass network. The structure of crystalline as well as amorphous B_2O_3 is made up of planar $[BO_{3/2}]^0$ triangles [24–26]. In amorphous B_2O_3, most of these triangles are arranged into boroxyl rings in which three oxygens are part of the ring

Table 1
Glass compositions, density (ρ), molar volume (M) and glass transition temperature (T_g)

Code	Li_2O (mol%)	ZnO (mol%)	B_2O_3 (mol%)	ρ (gm/cm^3)	M (cm^3)	T_g (K)
LB1	5	20	75	2.25	34.62	588
LB2	10	20	70	2.29	31.82	605
LB3	15	20	65	2.33	29.64	627
LB4	20	20	60	2.38	27.30	642
LB5	25	20	55	2.39	25.20	671
LB6	30	20	50	2.40	23.11	689

Table 2
Sound velocities (V_l and V_t), elastic moduli (L, G, E and K), Poisson's ratio (σ) and Debye temperature (θ_D)

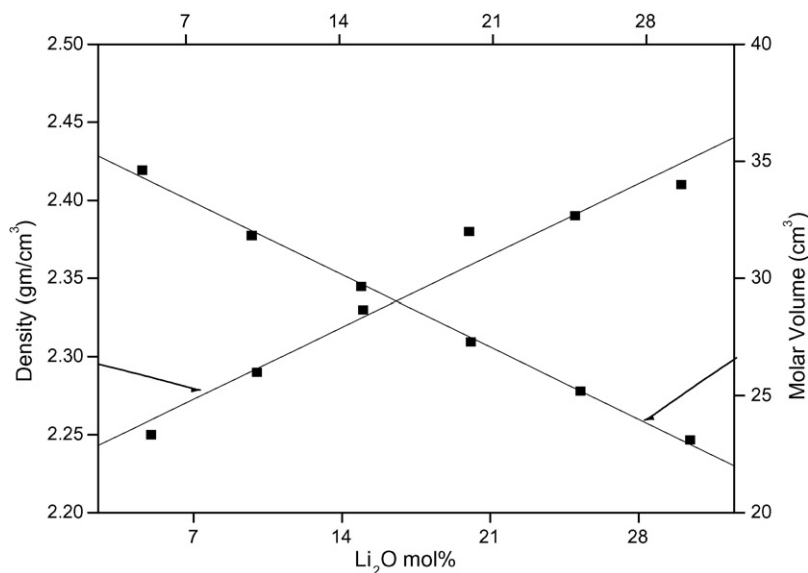| Code	V_l (m/s)	V_t (m/s)	L (GPa)	G (GPa)	E (GPa)	K (GPa)	σ	θ_D (K)
LB1	4318	2569	41.95	14.85	36.41	22.15	0.226	370
LB2	4759	2825	51.86	18.28	44.85	27.48	0.227	410
LB3	5295	3131	65.33	22.84	56.23	34.87	0.231	458
LB4	5644	3249	75.82	25.12	62.90	42.33	0.252	481
LB5	5901	3389	83.22	27.45	68.84	46.62	0.254	503
LB6	6308	3555	95.89	30.46	77.19	55.28	0.267	531

Fig. 1. Variation of density and molar volume with Li_2O mol%.

and three oxygens are outside the ring. These rings are randomly interconnected through loose $[BO_{3/2}]^0$ units. Due to the addition of modifying alkali oxide, such as Li_2O, Na_2O and K_2O, the three coordinated boron $[BO_{3/2}]^0$ units are converted to four coordinated boron tetrahedral $[BO_{4/2}]^-$ and thus the network dimensionality and connectivity increases [27,28]. This would lead to efficient packing and compactness in the structure.

The glass transition temperature (T_g) as a function of Li_2O concentration is shown in Fig. 2. It is a fact that T_g is a measure of structural degradation. In the present study, T_g increases with Li_2O mol%, indicating the conversion of three coordinated borons into four coordinated borons. The variation of T_g is not on the expected lines; actually T_g should decrease with increase of total modifier concentration above 33.3 mol%. In the present glass system even above 33.3 mol% of modifier content T_g monotonically increases. This could be due to the network-forming role of ZnO discussed in the following sections.
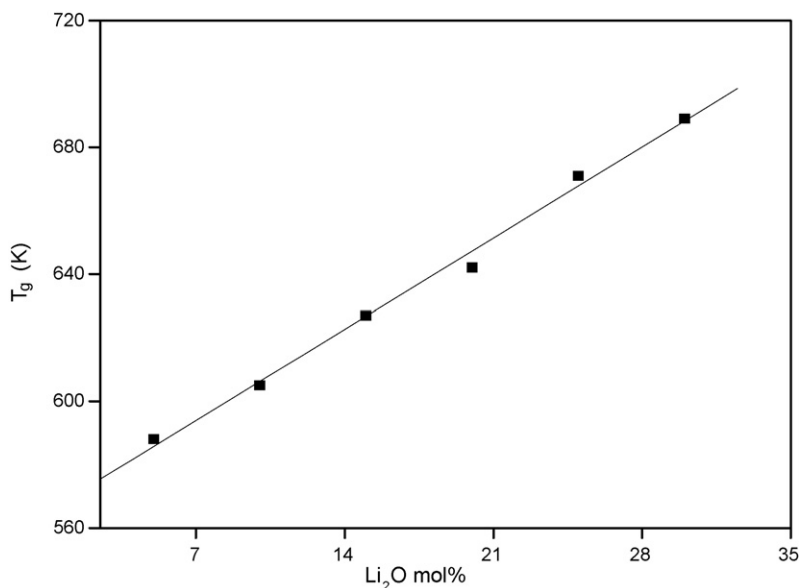

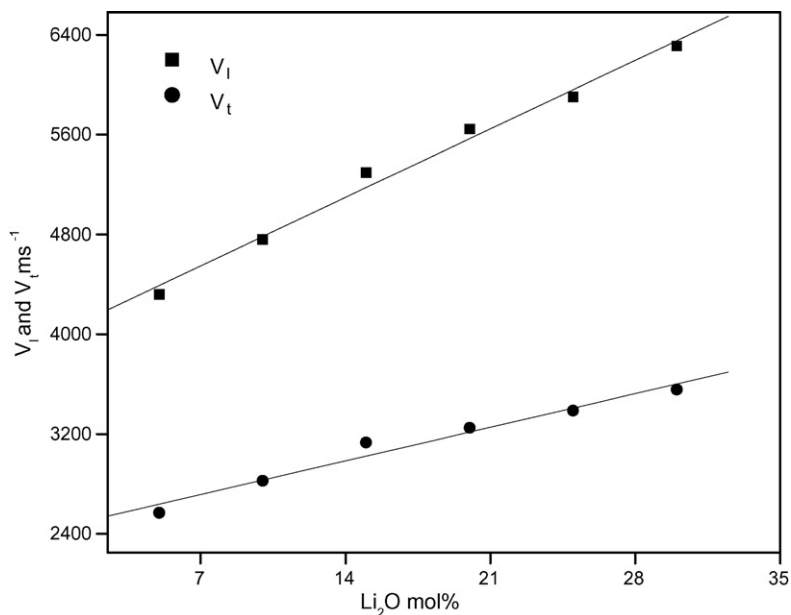Fig. 2. Variation of glass transition temperature with Li_2O mol%.

Fig. 3. Variation of sound velocities with Li_2O mol%.

3.2. Elastic properties

The compositional dependence of longitudinal (V_l) and transverse (V_t) sound velocities is shown in Fig. 3. The variation of elastic moduli as a function of Li_2O concentration is shown in Fig. 4. As can be seen from Figs. 3 and 4, both V_l, V_t and elastic moduli increase with the increase of Li_2O concentration over the entire range of composition.

This variation of ultrasound velocities and elastic moduli can be explained on the basis of the structural consideration of borate network. As pointed out in the earlier section, the vitreous B_2O_3 consists of planar $[BO_{3/2}]^0$
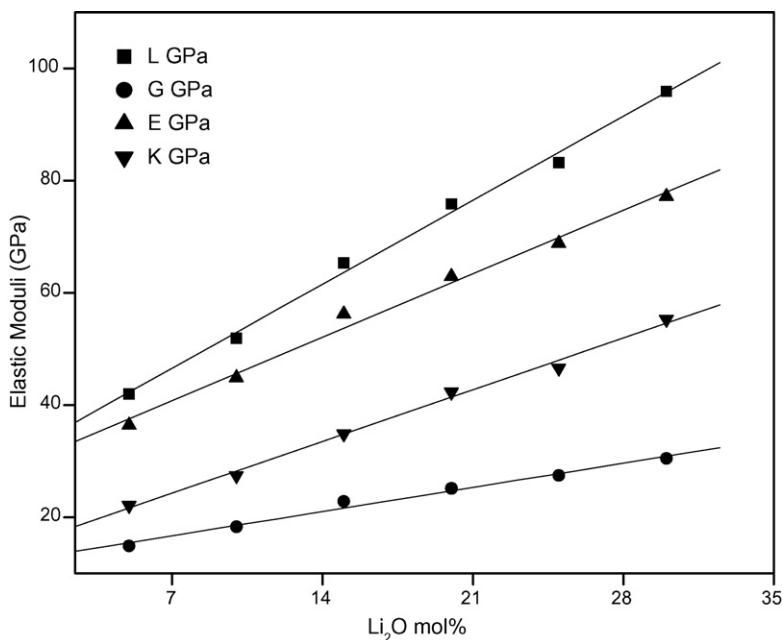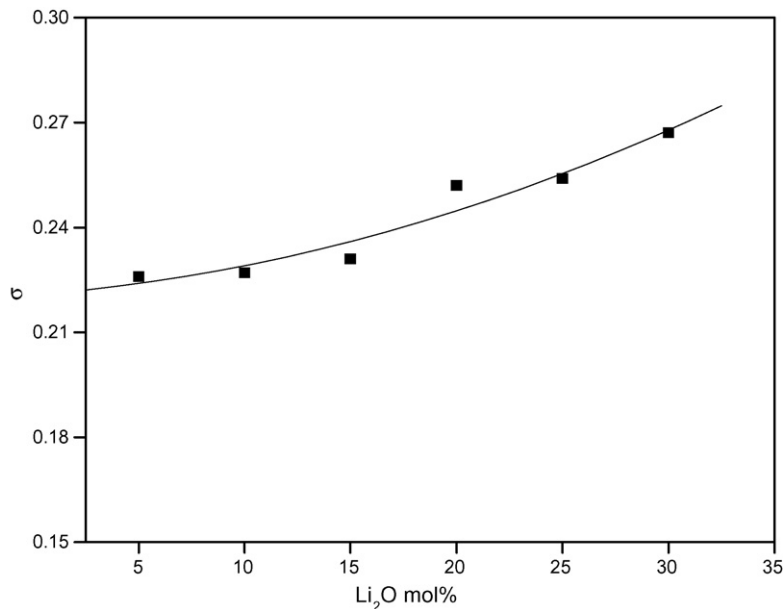

Fig. 4. Variation of elastic moduli with Li_2O mol%.

Fig. 5. Variation of Poisson's ratio with Li_2O mol%.

triangles [24,26]. The addition of alkali oxide to B_2O_3 network creates $[BO_{4/2}]^-$ units. This leads to increase in the network dimensionality and connectivity. We may define the dimensionality parameter as $D = 2y + 3(1 - y)$, where y is the concentration of $[BO_{3/2}]^0$ and $(1 - y)$ is the concentration of $[BO_{4/2}]^-$. Hence, both velocities and elastic moduli increase with the increase of Li_2O concentration. It may also be noted from Fig. 4 that the rate of change of elastic moduli is more pronounced in L and least in case of G. This indicates resistance to deformation and it is most probably due to presence of large number of covalent bonds [6,29,30].

We note here that N_4 reaches a maximum value of 0.5 (33.3 mol% of modifying oxide), above which $[BO_{4/2}]^-$ to $[BO_{3/2}]^0$ reconversion begins to occur [26] and this leads to loose structure because of the presence of non-
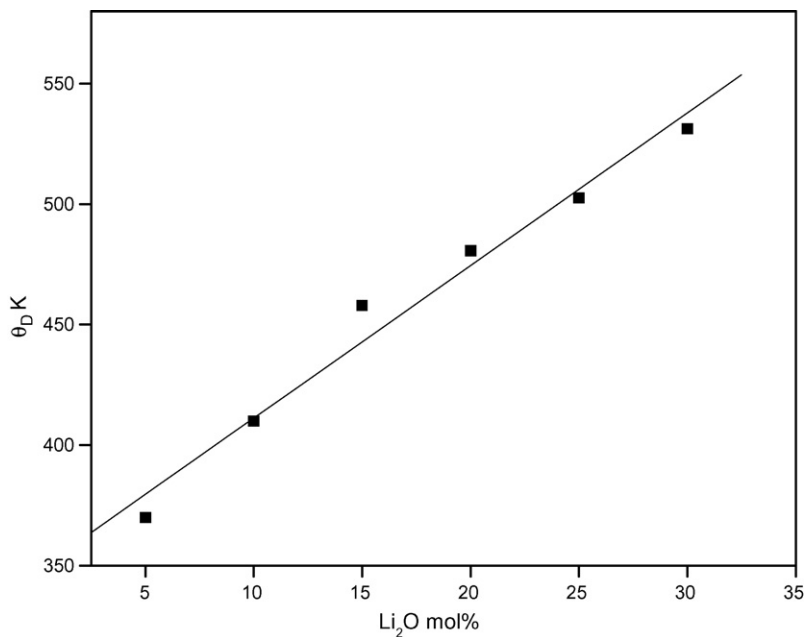

Fig. 6. Variation of Debye temperature with Li_2O mol%.

bridging oxygens (NBOs). In the present glass system if ZnO were to be incorporated into the network as a glass modifier, one would have expected decrease in both velocities and elastic moduli when the effective concentration of modifier oxide (Li$_2$O + ZnO) were to exceed 33.3 mol% [17]. Therefore, above 33.3 mol% of modifier concentration, the network consists of [BO$_{4/2}$]$^-$ tetrahedral along with [BO$_{3/2}$]^0 triangles. This strongly suggests that Zn^{2+} has utilized the excess of oxygens supplied by the modifier and it is likely to be incorporated into the network as a glass former.

Poisson's ratio and Debye temperature with Li$_2$O concentration is shown in Figs. 5 and 6, respectively. Poisson's ratio is the ratio of transverse and linear strains for a linear stress. Poisson's ratio has also been discussed in terms of the dimensionality of glass network. As the concentration of Li$_2$O increases [BO$_{3/2}$]^0 units are converted into [BO$_{4/2}$]$^-$ units. Increase in B$_4$ species results in enhancing the dimensionality of the network.

As it can be seen from Fig. 5, the Poisson's ratio is found to increase even when the effective concentration of modifier is greater than 33.3 mol%. This again suggests that there is no [BO$_{3/2}$]$^-$ groups formation with NBOs. Further, the values of Poisson's ratio are that of covalently bonded structure. The gradual increase of Debye temperature (see Fig. 6) also suggests increase in the compactness in the structure leading to increase in mean sound velocity [31].
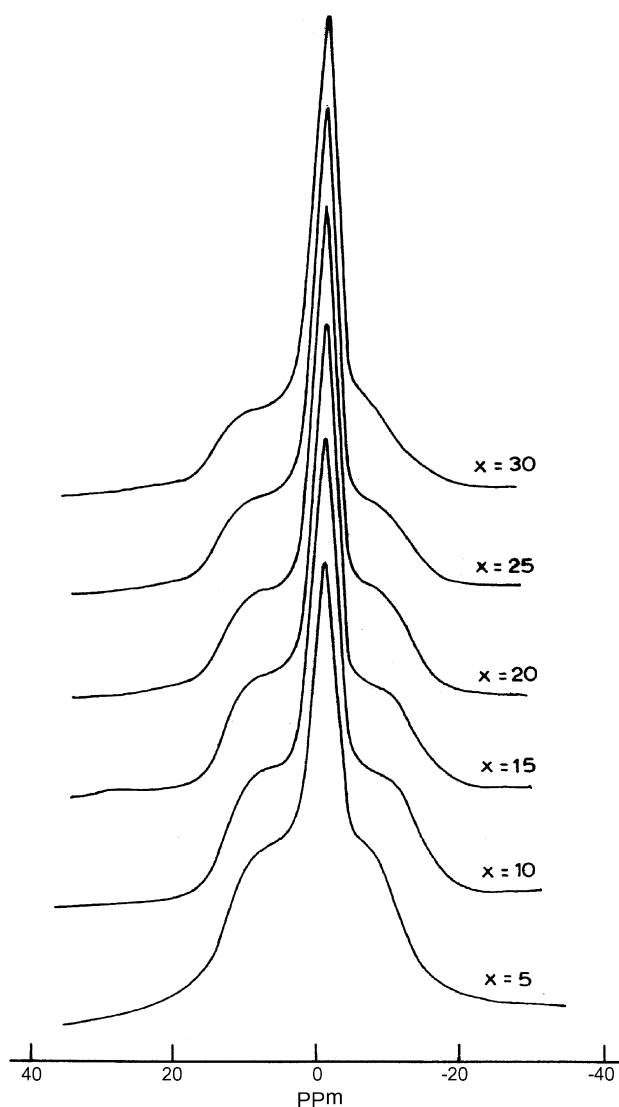

Fig. 7. ^{11}B MAS-NMR spectra of xLi$_2$O–20ZnO–(80 − x)B$_2$O$_3$ where (x = 5, 10, 15, 20, 25 and 30 mol%) glasses.
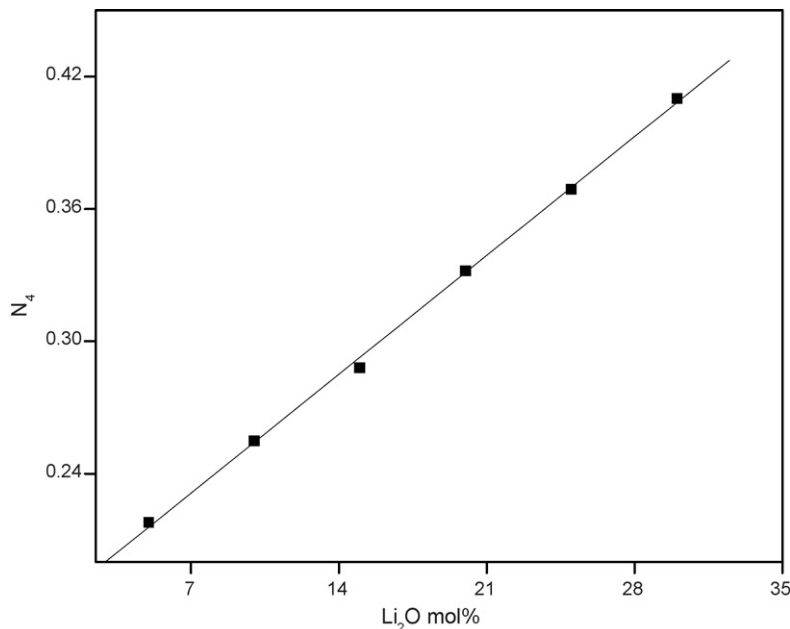
Fig. 8. Variation of N_4 with Li_2O mol%.

The above observation based on the elastic properties indicates that the Zn^{2+} ion prefers network-forming position and the observation seems to be consistent with the spectroscopic studies, which are discussed below.

3.3. ^{11}B MAS-NMR studies

^{11}B MAS-NMR spectra of $xLi_2O–20ZnO–(80 − x)B_2O_3$ where (x = 5, 10, 15, 20, 25 and 30 mol%) glass samples are shown in Fig. 7. The spectra reveal the presence of a sharp resonance peak at around −2 ppm (with respect to resonance signal of BF_3Et_2O), which arises from boron atom in four coordination $[BO_{4/2}]^-$ [25,32–35]. There is a split peak at the base of all the $[BO_{4/2}]^-$ signals which arises from boron atoms in three coordination $[BO_{3/2}]^0$ [32–34,36]. Fig. 6 shows that the intensities of $BO_{4/2}$ peak are found to increase with increase of Li_2O concentration at the expense of BO_3 peak. We have also examined variation of the fraction, N_4 [$N_4 = B_4/(B_3 + B_4)$] of boron atoms in $[BO_{4/2}]^-$ units by finding the area under the $[BO_{4/2}]^-$ and $[BO_{3/2}]^0$ peaks [37].

Fig. 8 shows the variation of N_4 as a function of Li_2O. As can be seen in figure the values of N_4 continuously increase with increase of Li_2O concentration and tend to reach the typical diborate composition value of $N_4 = 0.5$. This clearly suggests that the added oxygen supplied by Li_2O has been utilized for the formation of $[BO_{4/2}]^-$ groups. The scheme of modification can be represented as:

$$Li_2O \rightarrow O^{2-} + Li^+$$

$$[BO_{3/2}]^0 + \tfrac{1}{2}O^{2-} \rightarrow [BO_{4/2}]^-$$
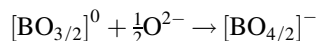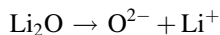
As pointed out in the earlier section, beyond the modifier (Li_2O + ZnO) concentration of 33.3 mol% the four coordinated boron atoms $[BO_{4/2}]^-$ are reconverted into $[BO_{3/2}]^0$ and one would expect decreasing trend in N_4. However, in the present glass system as seen from Fig. 8, such a trend has not been observed. This ascertains the fact that the excess of oxygens beyond 33.3 mol% of effective modifier concentration has not been utilized by B_2O_3 in the glass matrix. Therefore, it is possible that some of Zn^{2+} ions are present in the form of $[ZnO_{4/2}]^2$ tetrahedrons which can be represented by following scheme of reaction:
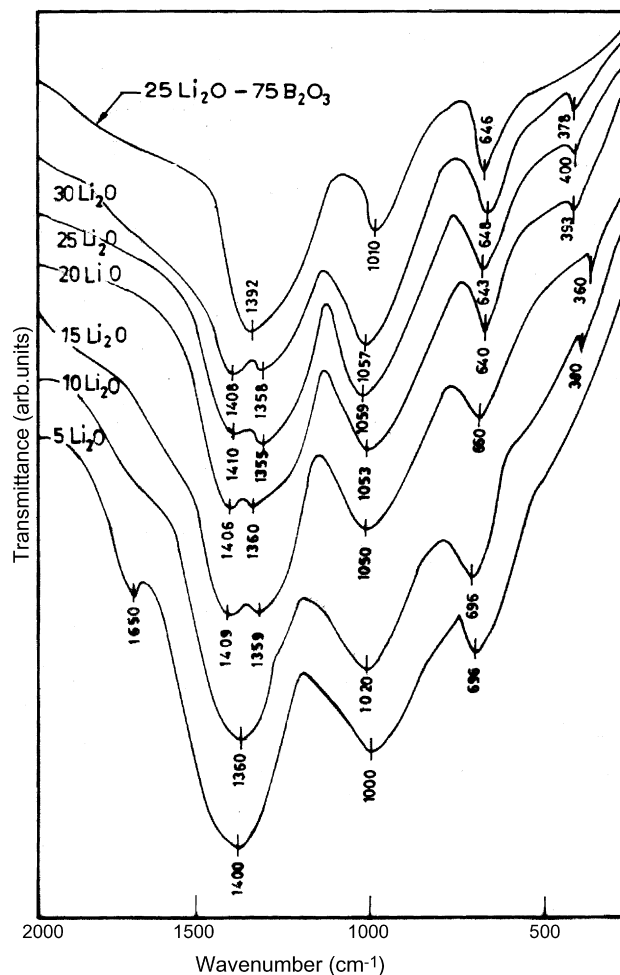
$$2ZnO \rightarrow [ZnO_{4/2}]^{2-} + Zn^{2+}.$$
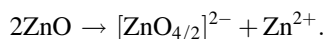
Fig. 9. Infrared spectra of binary $25Li_2O–75B_2O_3$ and ternary $xLi_2O–20ZnO–(80 − x)B_2O_3$ (x = 5, 10, 15, 20, 25 and 30 mol%) glasses.

Similar structural changes are known to occur in $Na_2O–MgO–B_2O_3$ [2] and $Li_2O–PbO–B_2O_3$ glasses [37], where the Mg/Pb ion is present in tetrahedral network positions.

3.4. Infrared spectral studies

The IR spectra of borate glasses occur mainly in three regions: those between 1200 and 1400 cm^{-1} which arise from borate units in which boron is connected to three oxygens (both bridging and non-bridging types, such as B_3^0 and B_2^-), those between 900 and 1100 cm^{-1} due to boron in tetrahedral oxygen coordination (B_4^-) and those peaks in the range 600–800 cm^{-1} due to the manifestation of B–O–B bending [8,38,39]. According to Tarte [40], ZnO tetrahedron $[ZnO_{4/2}]$ in glasses vibrate between 400 and 550 cm^{-1}.

Infrared spectra of representative compositions of the investigated glass system are shown in Fig. 9. The region between 1355 and 1410 cm^{-1} originates from the B−O stretching vibrations of B_3^0 and B_2^- species [40]. The region between 900 and 1100 cm^{-1} is due to boron atom in tetrahedra oxygen coordination $[BO_{4/2}]^-$ units [7,10,38]. The B–O–B bending vibrations manifest in the lower frequency region between 600 and 800 cm^{-1} [7,10,38]. The relative intensities of these peaks also undergo significant changes as Li_2O concentration increases. In the high frequency region (1640 cm^{-1}), an absorption peak is seen in one glass composition (borate rich), is attributed to the bending modes of –OH groups present due to the absorbed water [40]. The intensities of the peak at 1000 cm^{-1} corresponding to $[BO_{4/2}]^-$ units increases with increase of Li_2O concentration indicating an increase in formation of $[BO_{4/2}]^-$ units. In all the three regions, there is no significant frequency shifts. It is evident from

Fig. 9 that the absorption peaks become broader with the increase of Li_2O concentration, indicating greater disorderliness in the glass network [40]. The absorption bands in the range 398–410 cm^{-1} are likely to originate from the vibrational frequencies of $[ZnO_{4/2}]^{2-}$ tetrahedron, which is indicative of the incorporation of ZnO into the network-forming position.

4. Conclusions

Elastic properties, ^{11}B MAS-NMR and IR studies on Na_2O–ZnO–B_2O_3 glass system have been investigated to ascertain the role of Zn^{2+} ion in these glasses. The sound velocities, V_l and V_t, elastic properties, Poisson's ratio and Debye temperature show increasing trend even when the effective modifier concentration exceeds 33.3 mol%. The increase in Poisson's ratio suggests formation of weaker B–O–Zn linkages in place of strong B–O–B linkages. Analysis of ^{11}B MAS-NMR and IR spectra indicates that Zn^{2+} ions are incorporated into the network as a former presumably in the form of ZnO_4 tetrahedra.

Acknowledgements

References

[1] C.A. Angell, Solid State Ionics 9–10 (1983) 6.
[2] C.A. Angell, Chem. Rev. 90 (1990) 523.
[3] M. Ganguly, M. Harish Bhat, K.J. Rao, Mater. Res. Bull. 34 (1999) 1757.
[4] S. Greenblatt, P.J. Bray, Phys. Chem. Glasses 8 (1967) 213.
[5] K.S. Kim, P.J. Bray, Phys. Chem. Glasses 15 (1974) 47.
[6] B.G. Rao, H.G.K. Sundar, K.J. Rao, J. Chem. Soc. Faraday Trans. I80 (1984) 3491.
[7] E.I. Kamitsos, M.A. Karakassides, G.D. Chryssikos, Phys. Chem. Glasses 28 (1987) 203.
[8] E.I. Kamitsos, M.A. Karakassides, G.D. Chryssikos, J. Phys. Chem. 91 (1987) 1073.
[9] E.I. Kamitsos, G.D. Chryssikos, J. Mol. Struct. 247 (1991) 1.
[10] J. Krogh-Moe, Phys. Chem. Glasses 6 (1965) 46.
[11] R.V. Anavekar, N. Devaraj, G. Parthasarathy, E.S. Rajagopal, J. Ramakrishna, Phys. Chem. Glasses 30 (1989) 172.
[12] K.V. Damodaran, U.V. Selvaraj, K.J. Rao, Mater. Res. Bull. 23 (1988) 1151.
[13] E. Schreiber, O.L. Anderson, N. Soga, in: J. Robinson, S.E. Redka (Eds.), Elastic Constants and Their Measurement, The Kingsport Press, New York, 1973, p. 1.
[14] M. Kodama, J. Mater. Sci. 26 (1991) 4048.
[15] M. Kodama, T. Hirashima, T. Matsushita, Phys. Chem. Glasses 34 (1993) 130.
[16] M. Kodama, T. Matsushita, S. Kojima, Jpn. J. Appl. Phys. 34 (1995) 2570.
[17] J.T. Krause, C.R. Kurkjian, in: L.D. Pye, V.D. Frechette, N.J. reids (Eds.), Materials Science Research. Borate Glasses, vol. 12, Plenum Press, New York, Murray Hill, 1978, p. 577.
[18] S.V. Pakade, S.P. Yawale, W.J. Wawande, Acoust. Lett. 18 (1995) 212.
[19] S.P. Yawale, S.V. Pakade, C.S. Adgaonkar, Acoustica 76 (1992) 103.
[20] S.P. Yawale, S.V. Pakade, C.S. Adgaonkar, Acoustica 81 (1992) 184.
[21] A. Pal Singh, A. Paul, S. Bhatti, J. Pure Appl. Phys. 28 (1990) 483.
[22] H.J. Mcskimin, J. Acoust. Soc. Am. 33 (1961) 12.
[23] H.J. Mcskimin, P. Andreatch, J. Acoust. Soc. Am. 34 (1962) 609.
[24] P.J. Bray, J. Non-Cryst. Solids 75 (1985) 29.
[25] P.J. Bray, in: E. Porai-Koshits (Ed.), The Structure of Glass, Consultant Bureau, New York, 1996.
[26] P.J. Bray, J.G. O'Keefe, Phys. Chem. Glasses 4 (1963) 37.
[27] B. Warren, J. Am. Ceram. Soc. 24 (1941) 256.
[28] T. Abe, J. Am. Ceram. Soc. 35 (1952) 756.
[29] B. Wang, S.P. Szu, M. Greenblatt, J. Non-Cryst. Solids 134 (1991) 249.
[30] K.V. Damodaran, K.J. Rao, J. Mater. Sci. 24 (1989) 2380.
[31] K.V. Damodaran, K.J. Rao, J. Am. Ceram. Soc. 72 (1989) 533.
[32] A.H. Silver, P.J. Bray, J. Chem. Phys. 29 (1958) 984.
[33] J. Zhong, P.J. Bray, J. Non-Cryst. Solids 111 (1989) 67.
[34] S. Muthupari, K.J. Rao, J. Phys. Chem. 98 (1994) 2646.
[35] S. Prabakar, K.J. Rao, C.N.R. Rao, Proc. R. Soc. (Lond.) A429 (1990) 1.

[36] S. Prabakar, K.J. Rao, C.N.R. Rao, Eur. J. Solid State Inorg. Chem. 29 (1992) 95.

[37] M. Ganguly, M. Harish Bhat, K.J. Rao, J. Phys. Chem. B103 (1999) 920.

[38] U. Selvaraj, K.J. Rao, Spectrochim. Acta A40 (1984) 1081.

[39] V.C. Veeranna Gowda, R.V. Anavekar, Ionics 10 (2004) 103.

[40] P. Tarte, Bull. Soc. Fr. Ceram. 58 (1963) 13.